

Supporting Information

for

Rapid Mechanochemical Preparation of a Sandwich-like Charge Transfer Complex

Hao Chen, Fan Gao, Erdong Yao, Qi Chen, Yuguo Ma*

Beijing National Laboratory for Molecular Sciences (BNLMS), Key Lab of Polymer Chemistry & Physics of Ministry of Education, College of Chemistry, Peking University, Beijing 100871, China

Email: ygma@pku.edu.cn

Table of Contents

	Page
1. Experimental Section	S2
2. ^1H NMR, ^{13}C NMR, ^{19}F NMR Spectra	S4
3. Solid-state ^{13}C NMR Spectra	S10
4. Emission Spectra and UV-Vis absorption spectra	S11
5. Electrochemical Characterizations	S12
6. Computational Studies	S13
7. X-ray Diffraction Pattern	S14
8. Crystal Data and Structure Refinement	S16

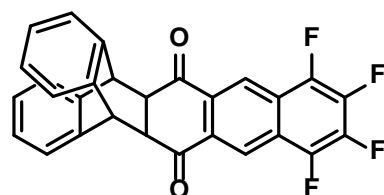
1. Experimental Section

General Methods: Chemicals were purchased commercially and used without further purification. All air and moisture sensitive reactions were performed under a nitrogen (N_2) atmosphere using standard Schlenk techniques. Toluene was freshly distilled from sodium under N_2 prior to use. 1H and ^{19}F NMR spectra were recorded on a Varian Mercury-300 (300 MHz) or Bruker-400 (400 MHz) spectrometer, and ^{13}C spectra were recorded on a Bruker-400 (400 MHz) spectrometer using $CDCl_3$ as solvent. Chemical shifts are reported in parts per million (ppm) and coupling constants are reported in hertz (Hz). 1H NMR chemical shifts were referenced versus TMS (0 ppm), ^{13}C NMR chemical shifts were referenced versus $CDCl_3$ (77.16 ppm) and ^{19}F NMR chemical shifts were referenced versus a CF_3CO_2H external standard (0 ppm). Solid-state NMR spectrum of CT complex **1** was recorded on BRUKER AVANCE III 400M spectrometer (FT, 100 MHz for ^{13}C). High-resolution mass spectra (HRMS) were recorded on a Bruker Apex IV FTMS mass spectrometer using ESI (electrospray ionization). Cyclic voltammograms (CVs) were recorded on a CHI706A electrochemical analyzer using glassy carbon discs as the working electrode, Pt wire as the counter electrode, Ag/AgCl electrode as the reference electrode, and ferrocene/ferrocenium as an internal reference. The scan speed was 100 mV/s. A solution of tetrabutylammonium hexafluorophosphate (TBAPF₆) in CH_2Cl_2 (0.1 M) was employed as the supporting electrolyte. Powder X-ray diffraction data was collected on a PHILIPS X’Pert Pro diffractometer with an X’celerator detector in the reflection mode at 30 °C, using monochromatized Cu K α radiation. Single crystal

X-ray diffraction data was collected with a NONIUS Kappa CCD diffractometer for CT complex **1**, with graphite monochromator and Mo K α radiation [λ (MoK α) = 0.71073 Å]. Structures were solved by direct methods with SHELXS-97 and refined against F² with SHELXS-97.

Mechanochemistry: in a typical experiment, 36 mg (0.2 mmol) of **AN** and 112 mg (0.4 mmol) of **TFAQ** were placed in a mortar and ground for 10 min with few drops hexane added. Solvent-free manual grinding was also carried out and showed the CT complex formation from the change of color, which required about half an hour.

Compound **TFAQ** was synthesized according to reference.^[1]



Adduct 2

Adduct 2: A Schlenk-adapted tube was charged with 90 mg (0.5 mmol) of **AN** and 62 mg (0.22 mmol) of **TFAQ**, 3 mL of toluene under nitrogen atmosphere. After stirred for 40 h at 110 °C, the solvent was removed under reduced pressure, and the residue was purified by flash column chromatography over silica gel, to afford the product as a yellow solid (66 mg, 0.144 mmol, 66 %)

¹H NMR (400 MHz, CDCl₃, ppm): δ 8.61(s, 2H), 7.47 (m, 2H), 7.23 (m, 2H), 7.12 (m, 2H), 6.80 (m, 2H), 5.05 (s, 2H), 3.48 (s, 2H), ¹³C NMR (100 MHz, CDCl₃, ppm): δ

195.7, 144.4, 141.9 ($J_{C-F} = 250$ Hz), 141.8, 141.2, 138.7 ($J_{C-F} = 250$ Hz), 139.9, 131.8, 126.7, 126.4, 124.7, 123.9, 121.3, 121.2, 50.4, 49.4. ^{19}F NMR (282 MHz, CDCl_3 , ppm): δ -74.3, -80.5. HR-MS (CDCl_3 , $\text{C}_{28}\text{H}_{14}\text{F}_4\text{O}_2$, m/z): Found: 481.08305 (M^+), Cal: 481.08221, Error: 0.8 mDa

2. ^1H NMR, ^{13}C NMR, ^{19}F NMR Spectra

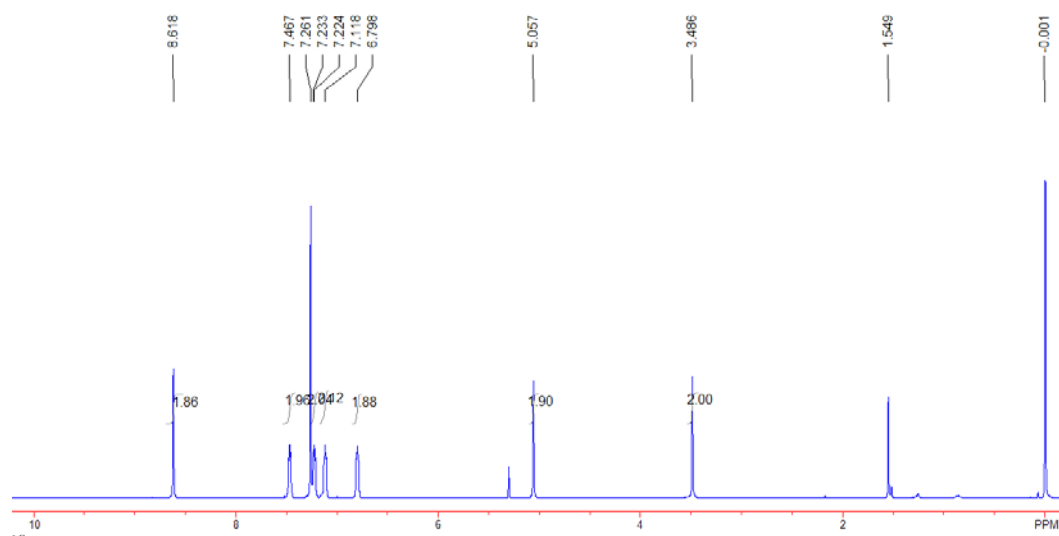


Figure S1. ^1H NMR spectrum of adduct **2** in CDCl_3 .

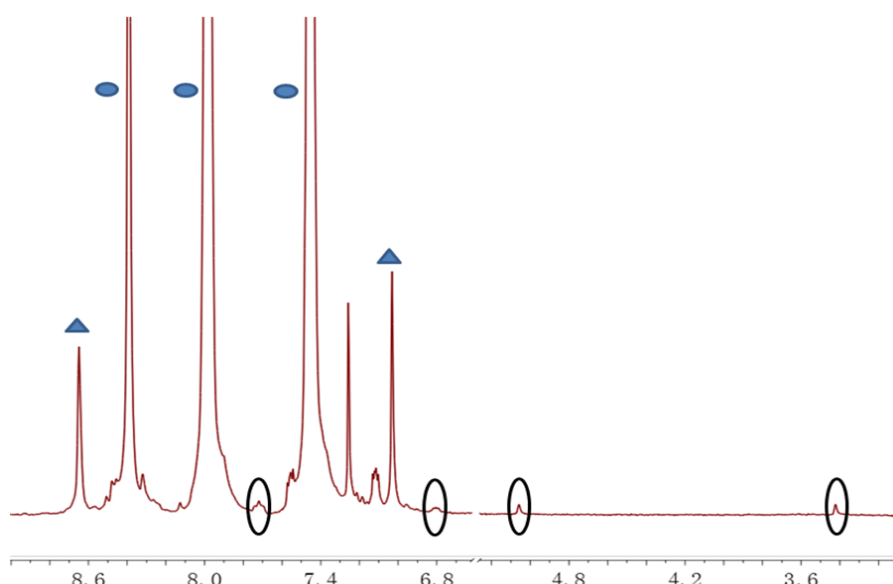


Figure S2. Partial ^1H NMR spectrum (in CDCl_3) of crude product (AN indicated by

blue oval and **TFAQ** indicated by blue triangle) containing trace amount of adduct **2** (indicated by the black circle) from heating a 1:9 binary mixture of CT complex **1** and **AN** (Figure 3c).

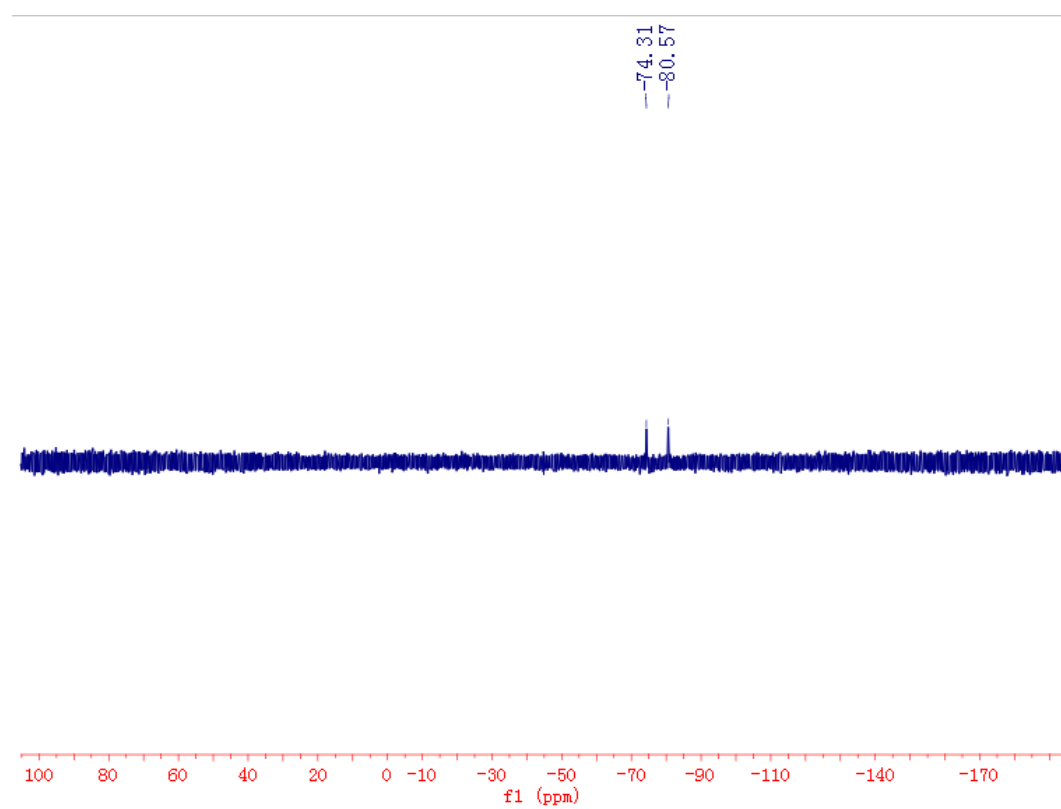


Figure S3. ¹⁹F NMR spectrum of adduct **2** in CDCl₃

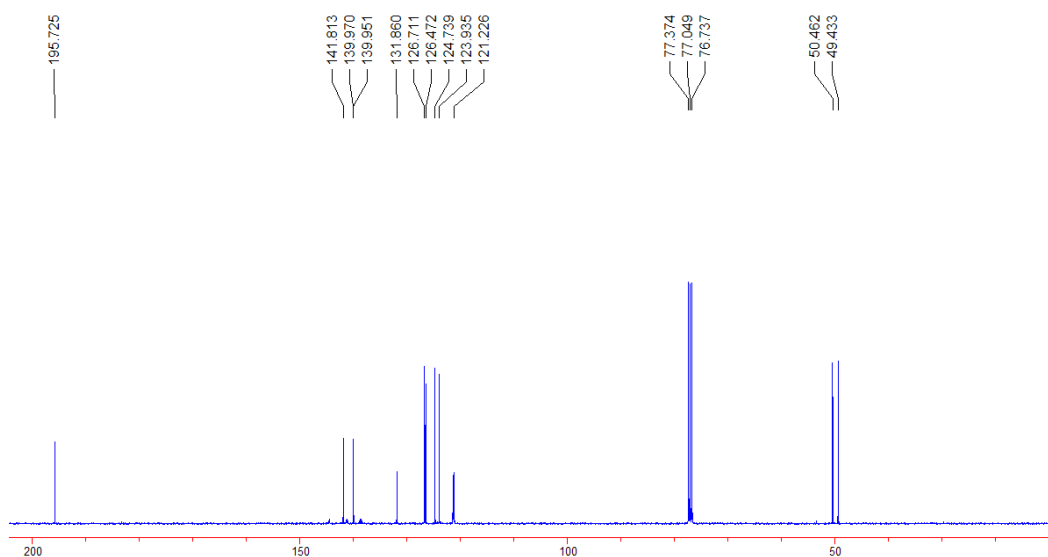


Figure S4. ¹³C NMR spectrum of adduct **2** in CDCl₃

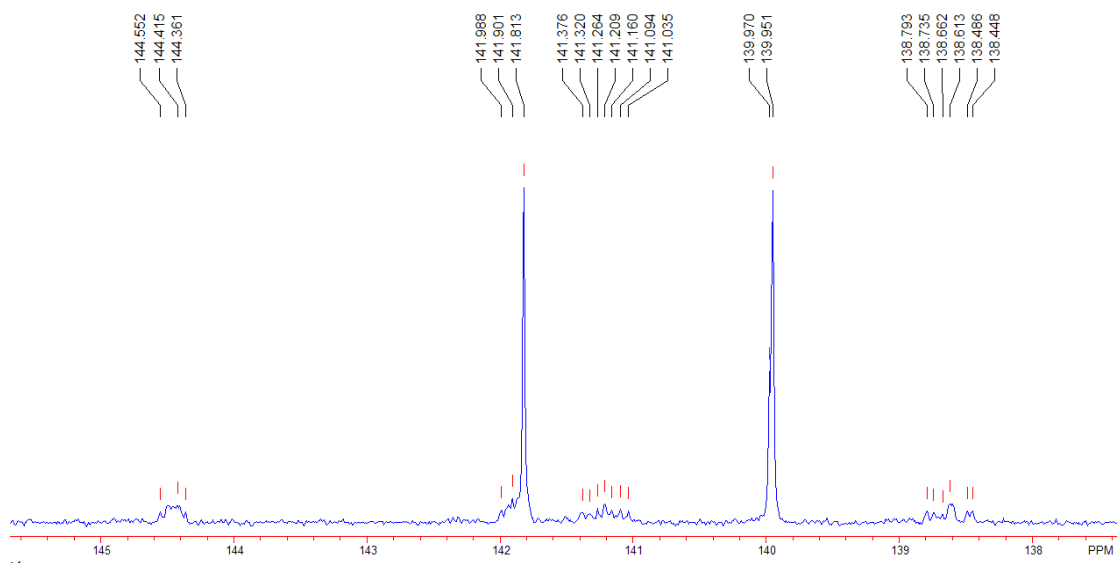


Figure S5. Partial ¹³C NMR spectrum of adduct **2** in CDCl_3

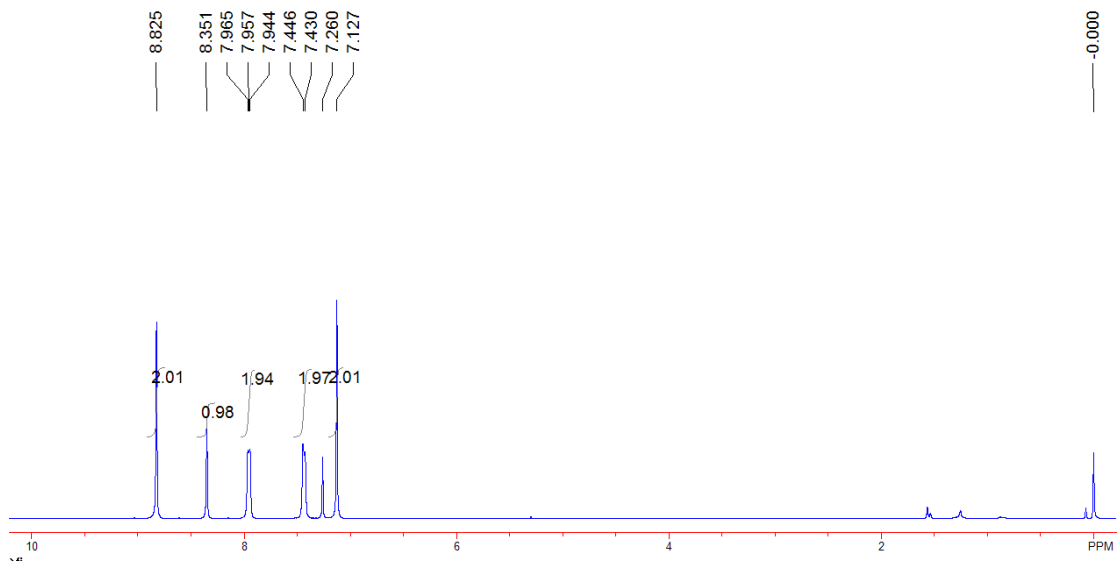


Figure S6. ¹H NMR spectrum of CT complex **1** (grown from solution of **AN** and **TFAQ**) in CDCl_3

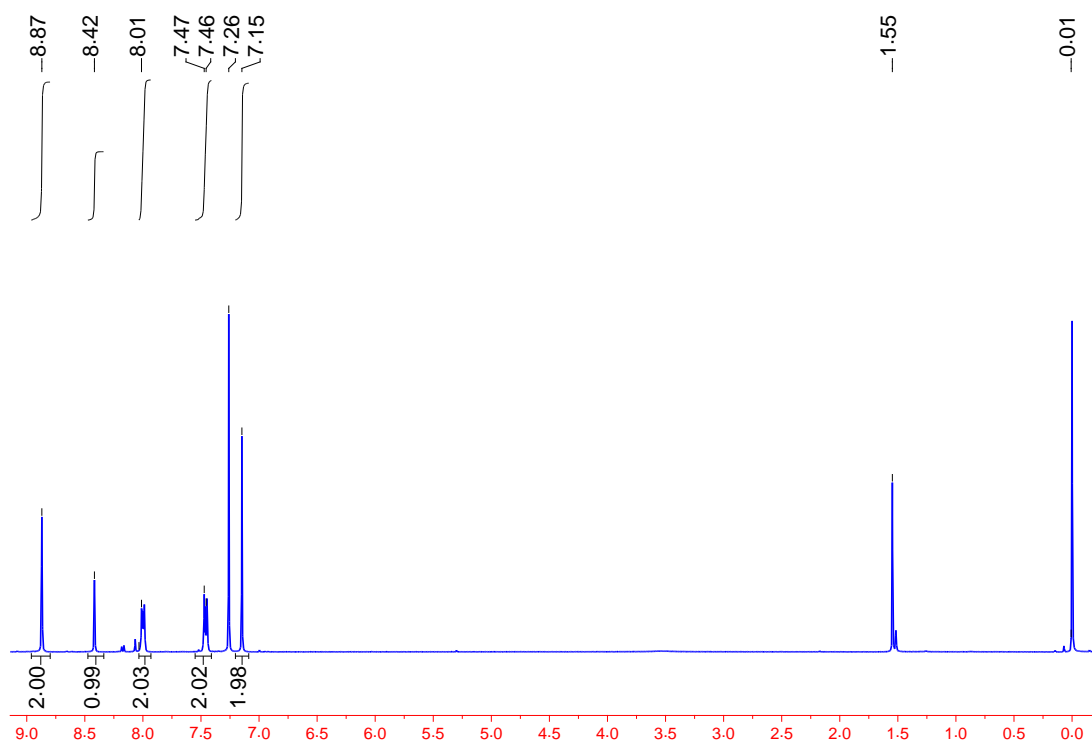


Figure S7. ^1H NMR spectrum of CT complex **1** (grown from solution of **AN**, pyrene, naphthalene and **TFAQ**) in CDCl_3

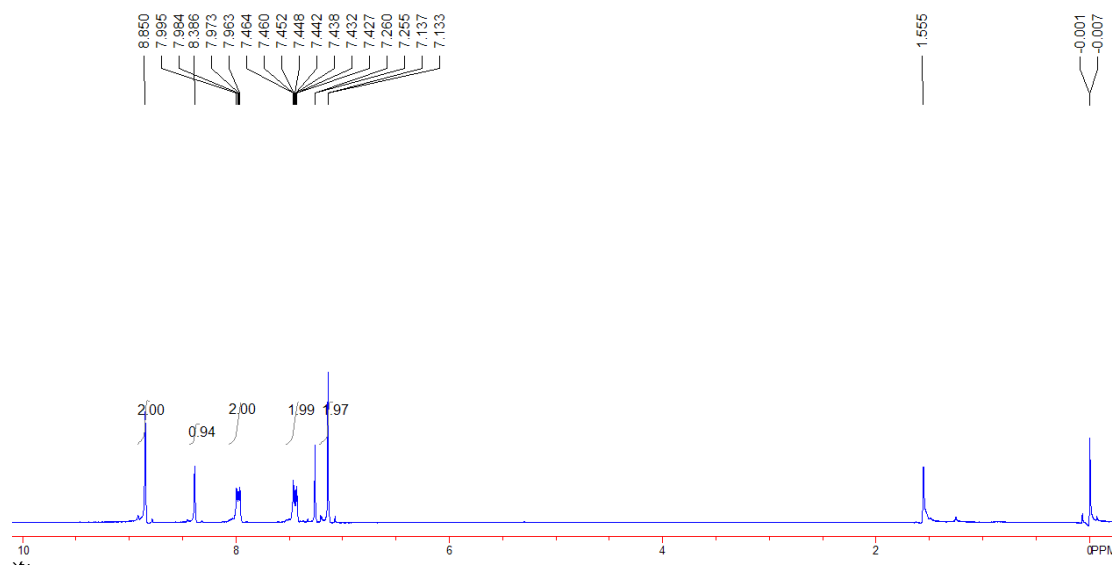


Figure S8. ^1H NMR spectrum of CT complex **1** (quickly precipitate from mixing the concentrated chloroform solutions of **AN** and **TFAQ**) in CDCl_3 .

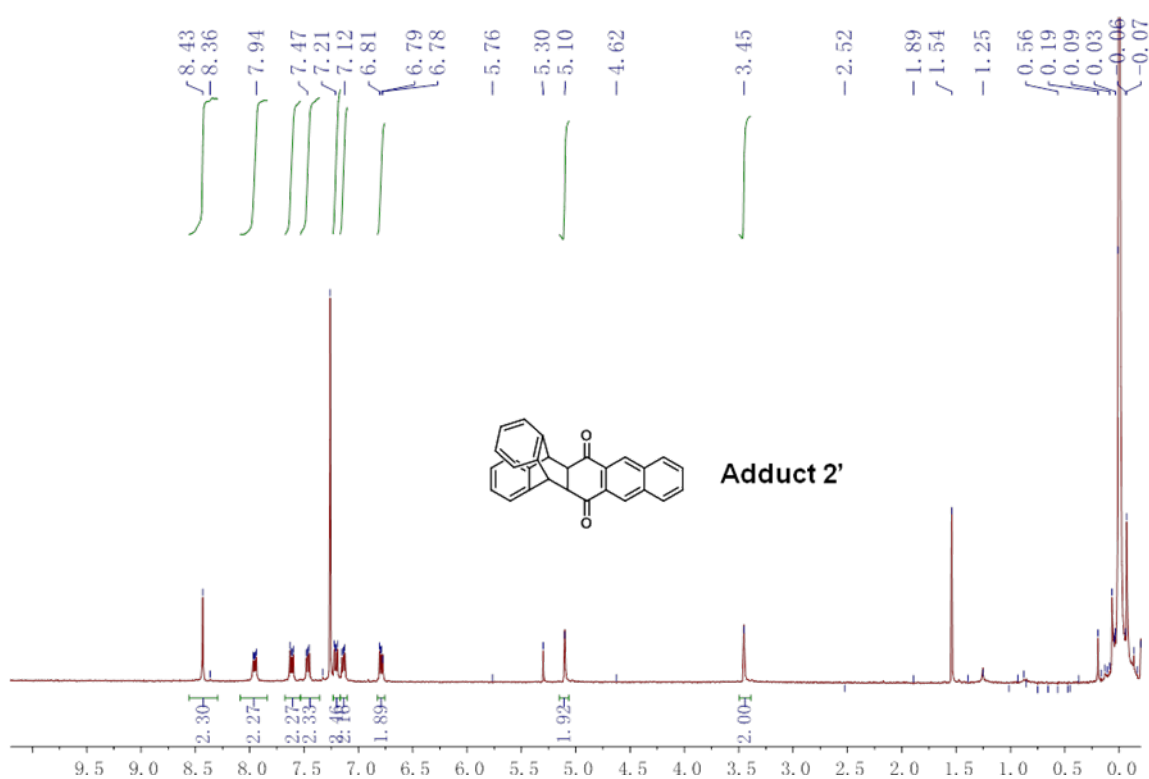


Figure S9. ^1H NMR spectrum of adduct $\mathbf{2}'$ in CDCl_3 .

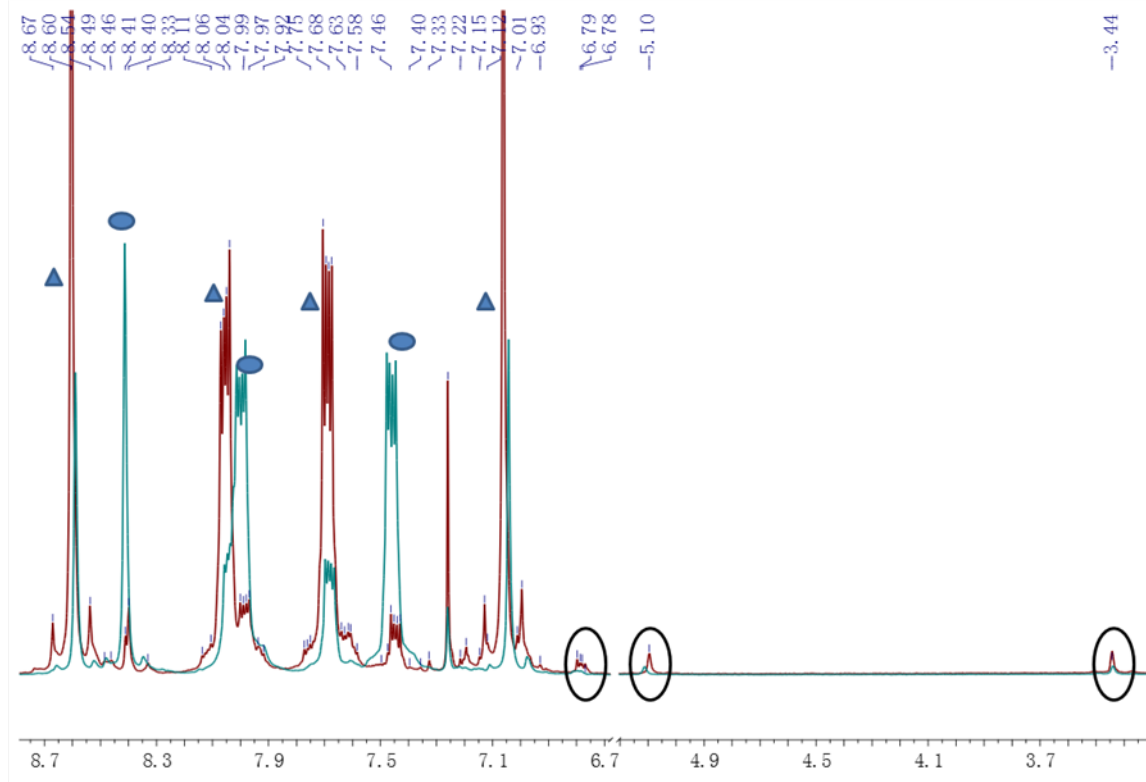


Figure S10. Partial ^1H NMR spectrum (in CDCl_3) of crude product (AN indicated by blue oval and AQ indicated by blue triangle) containing adduct $\mathbf{2}'$ (indicated by the

black circle) from heating a 1:5 after-grinding binary mixture of **AQ** and **AN** (blue line) and a 2:1 after-grinding binary mixture of **AQ** and **AN** (red line).

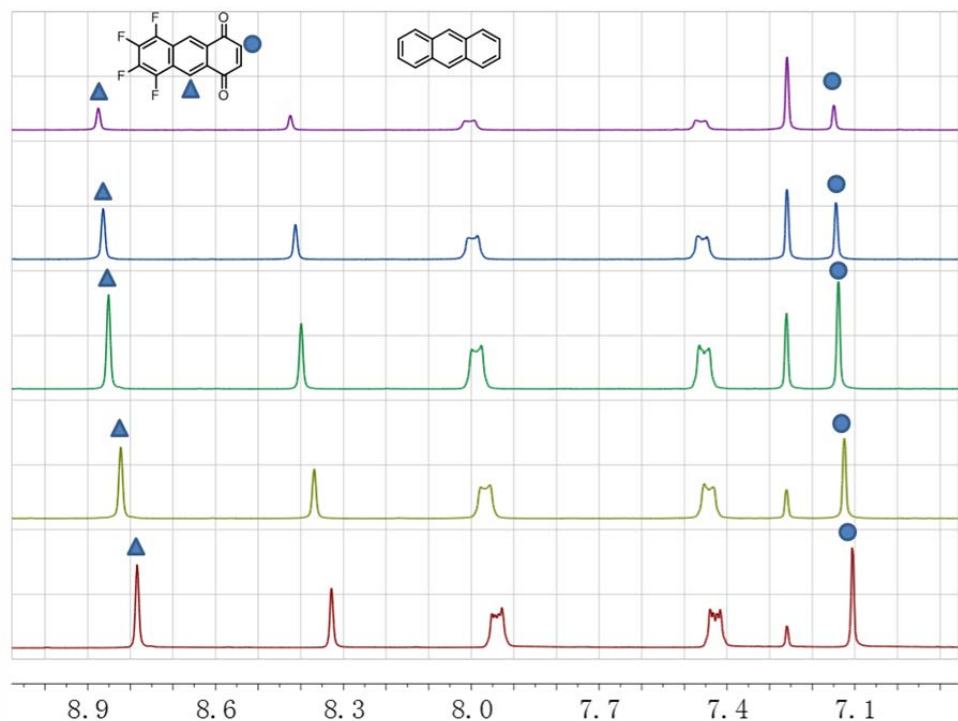


Figure S11. Variable concentration ^1H NMR spectrums of **AN** and **TFAQ**. From bottom to top, the concentration of **AN** is $3.5 \times 10^{-2} \text{ M}$, $1.8 \times 10^{-2} \text{ M}$, $9.0 \times 10^{-3} \text{ M}$, $4.5 \times 10^{-3} \text{ M}$, $2.2 \times 10^{-3} \text{ M}$, respectively, while concentration of **TFAQ** is $7 \times 10^{-2} \text{ M}$, $3.5 \times 10^{-2} \text{ M}$, $1.8 \times 10^{-2} \text{ M}$, $9 \times 10^{-3} \text{ M}$, $4.5 \times 10^{-3} \text{ M}$, respectively.

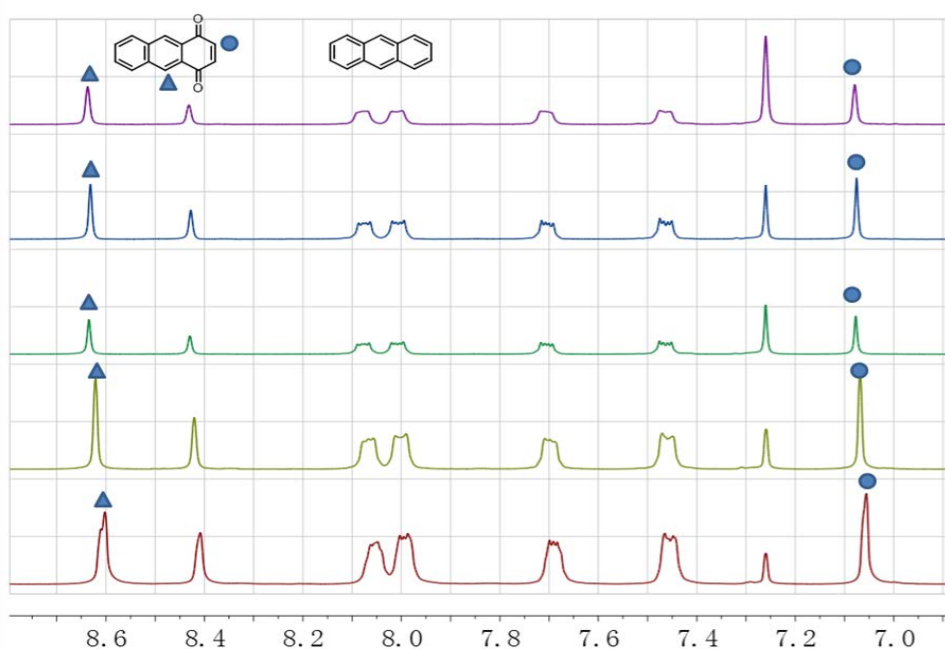


Figure S12. Variable concentration ¹H NMR spectrums of **AN** and **AQ**. From bottom to top, the concentration of **AN** is 3.5×10^{-2} M, 1.8×10^{-2} M, 9.0×10^{-3} M, 4.5×10^{-3} , 2.2×10^{-3} M, respectively, while concentration of **AQ** is 7×10^{-2} M, 3.5×10^{-2} M, 1.8×10^{-2} M, 9×10^{-3} , 4.5×10^{-3} M, respectively.

3. Solid-state ¹³C NMR spectra

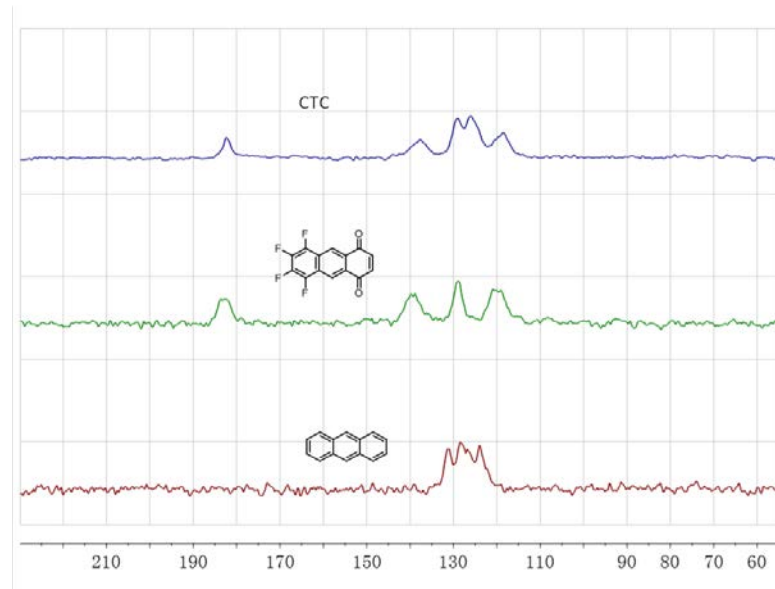


Figure S13. Solid-state ¹³C NMR spectrums of **1**, **TFAQ** and **AN**.

4. Emission Spectra and UV-vis absorption spectra

UV-Vis absorption spectra were recorded on a Hitachi U-4100 spectrophotometer using the absorption mode in a 1 cm quartz cell and 1 cm quartz plate. Fluorescence emission spectra were recorded in 1 cm quartz cuvette and 1 cm quartz plate for solid samples on a Horiba Jobin Yvon FluoroMax-4P spectrofluorometer. The emission spectra were corrected for the wavelength dependence of detector sensitivity and monochromator gratings.

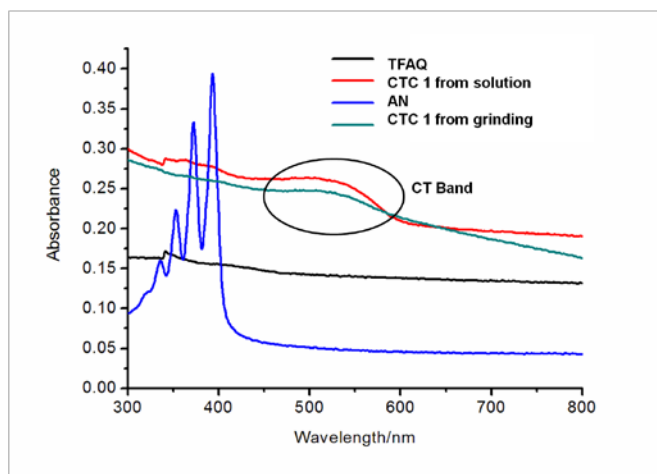


Figure S14. UV-Vis spectra in solid state: blue, black, red and green lines correspond to **AN**, **TFAQ**, CT complex **1** grown from solution and **1** from grinding, respectively.

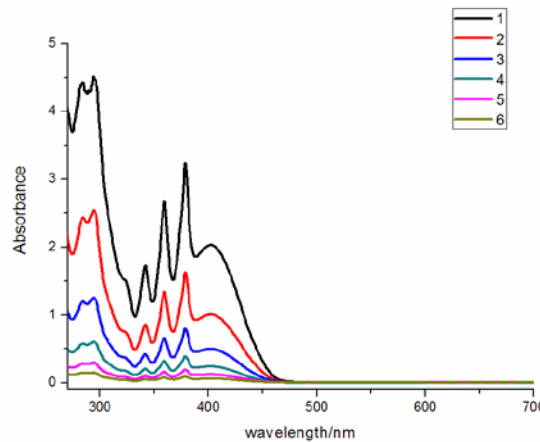


Figure S15. Variable concentration UV-Vis spectra of **1** in CHCl_3 solution (from the top to bottom, the concentration of **AN** is 2×10^{-4} , 1×10^{-4} , 5×10^{-5} , 2.5×10^{-5} , 1.25×10^{-5} , 6×10^{-6} M, respectively, while concentration of **TFAQ** is 4×10^{-4} , 2×10^{-4} , 1×10^{-4} , 5×10^{-5} , 2.5×10^{-5} , 1.25×10^{-5} M, respectively.)

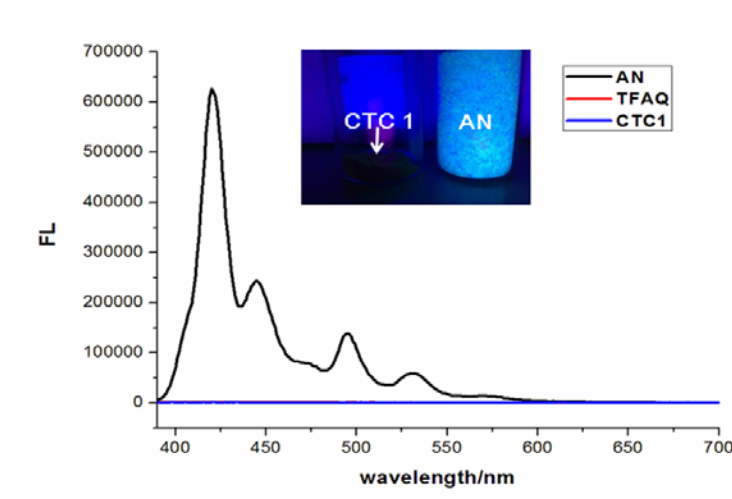


Figure S16. Fluorescence emission spectra of **AN**, **TFAQ** and **1** in solid state (excited at 372 nm). (Inset: the photo of **AN** and **CTC 1** in solid state excited at 365 nm).

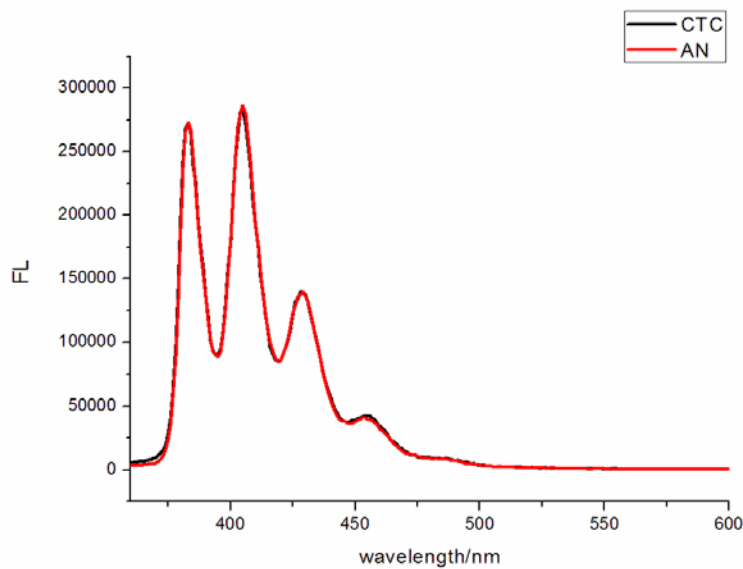


Figure S17. Fluorescence emission spectra of **AN** (red line) and **1** (black line) in CHCl_3 solution (both of the concentration of **AN** are 6×10^{-6} M). (excited at 341 nm).

5. Electrochemical Characterizations

The energy level of Fc/Fc^+ is assumed to be -4.8 eV below the vacuum level.^[2,3] The LUMO levels of **AQ** and **TFAQ** were estimated from the half-wave potentials of the reduction peaks. The half-wave potential of oxidation peak of **Fc** was measured to be

0.43 V against Ag/AgCl.

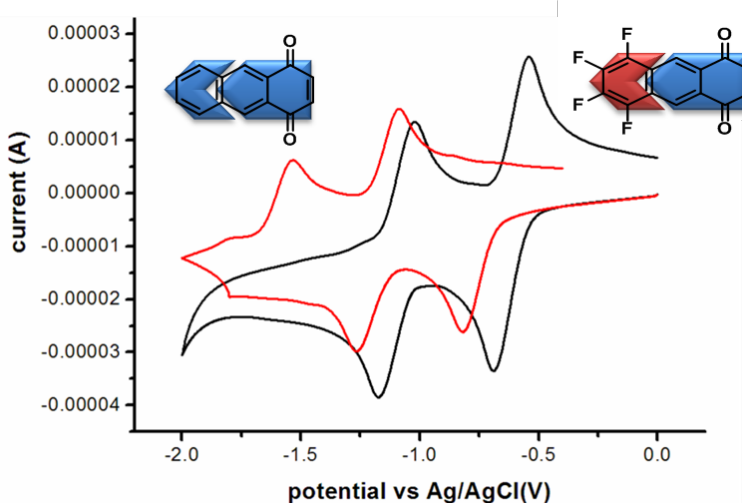


Figure S18. CVs of **AQ** and **TFAQ**.

6. Computational Studies

The geometry of the molecules was optimized with Density Functional Theory (DFT) using B3LYP hybrid functional⁴ with a basis set limited to 6-31g*. Molecular orbital shapes and energies were obtained at optimized geometries. Calculation was performed with the Gaussian03⁵ package and the orbital pictures were prepared using Gaussview.⁶

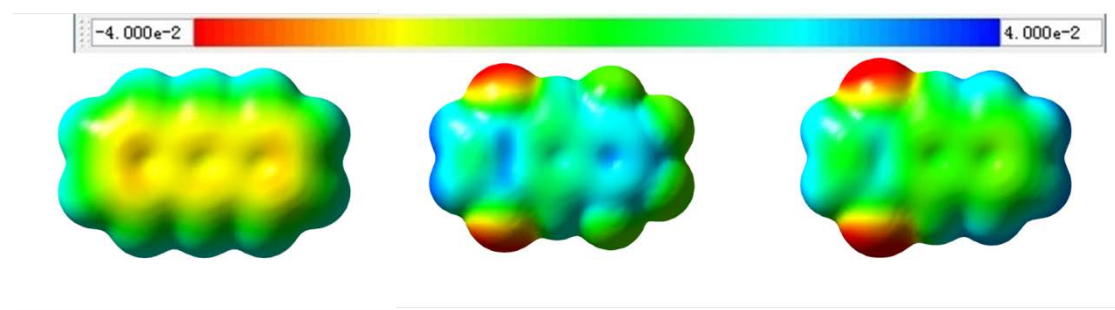


Figure S19. DFT calculated electrostatic potential (ESP) of **AN**, **TFAQ** and **AQ** in the same scale (from left to right)

The ESP plots of **AN**, **TFAQ** and **AQ** revealed that **TFAQ** had the most positive π clouds, while **AN** had the least and matched **TFAQ** best.

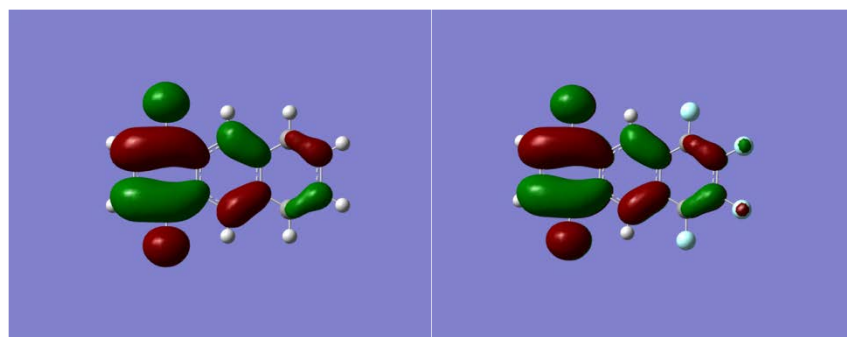


Figure S20. DFT calculated LUMO of **AQ** (left) and **TFAQ** (right).

Table S1. Summary of electronic data in DCM in comparison with calculated results

Comp.	AQ	TFAQ
LUMO (eV) ^a	-3.4	-3.7
LUMO (eV) ^b	-3.0	-3.3

^a calculated based on CV; ^b calculated based on DFT calculation (The HOMO of **AN** is -5.2 eV , which is calculated based on DFT calculation).

7. X-ray Diffraction Pattern

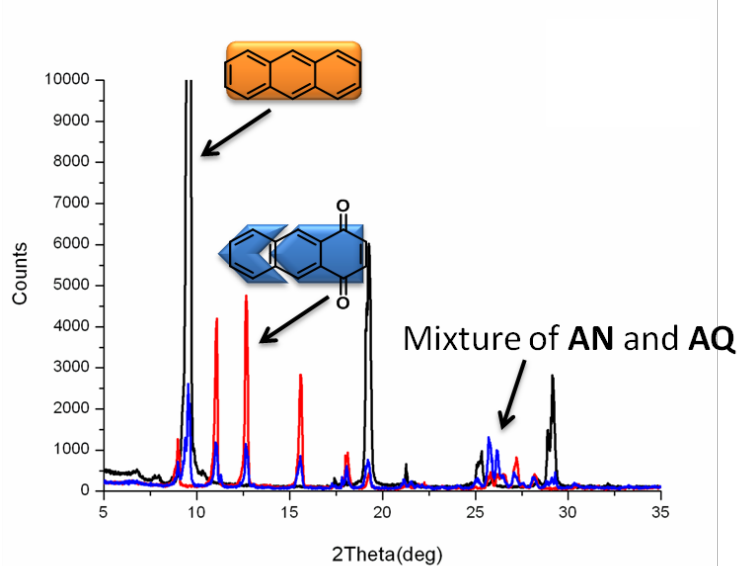


Figure S21. X-ray diffraction patterns of **AN**, **AQ**, mixture of **AN** and **AQ**.

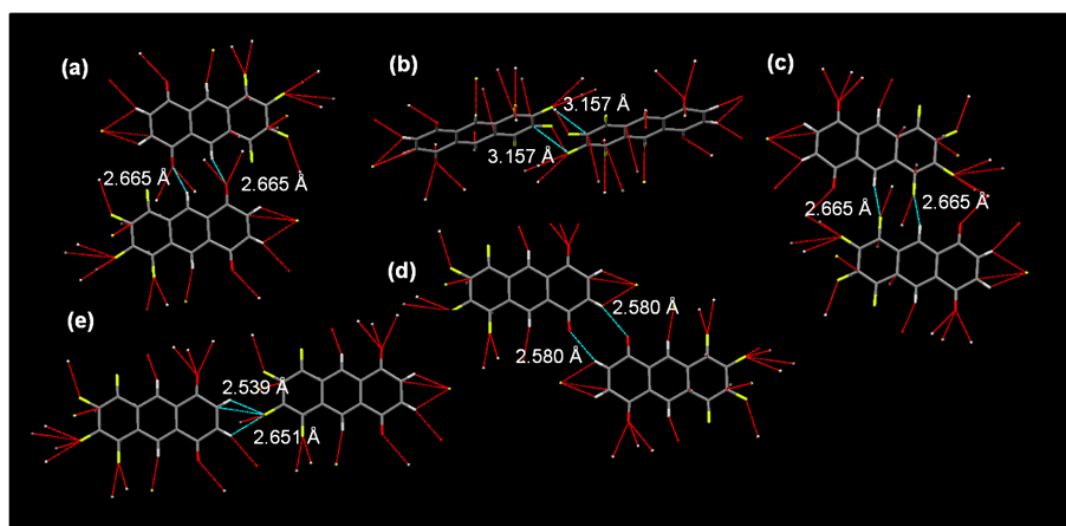


Figure S22. Weak C-H…F and C-H…O interactions between two neighbouring **TFAQ** molecules in the crystal structure of CT complex **1**.

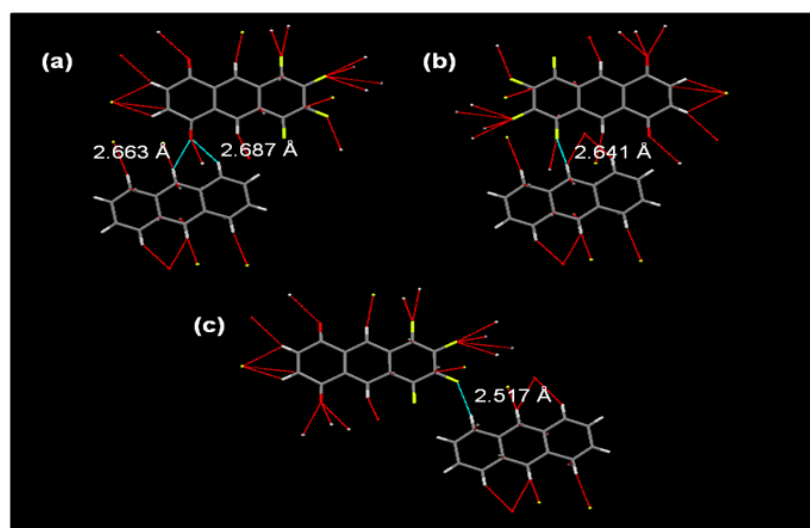


Figure S23. Weak C-H…F and C-H…O interactions between two neighbouring **TFAQ** and **AN** molecules in the crystal structure of **1**.

The CH…F distances are 2.665 Å, 2.539 Å, 2.651 Å, 2.641 Å and 2.517 Å, respectively, for contacts shown in Figure S14c,e and S15b,c. The sum of van der Waals radii of H and F is 2.56 Å,⁷ indicating the existence of a favorable CH…F interaction. The CH…O distances are 2.655 Å, 2.580 Å, 2.663 Å and 2.687 Å, respectively, for contacts shown in Figure S14a,d and S15a. The sum of van der Waals radii of H and O is 2.68 Å,⁷ indicating the existence of a favorable CH…O interaction. Also C…F interactions can be observed in Figure S14b,e. The sum of van der Waals radii of C and F is 3.23 Å.⁷

8. Crystal Data and Structure Refinement

Table S2-1 Crystal data and structure refinement for CT complex **1**.

Identification code	1		
Empirical formula	$C_{21}H_9F_4O_2$		
Formula weight	369.28		
Temperature	173(2) K		
Wavelength	0.71073 Å		
Crystal system, space group	Triclinic, P-1		
Unit cell dimensions	$a = 8.3985(17)$ Å	$\alpha = 70.94(3)$ deg.	
	$b = 9.819(2)$ Å	$\beta = 81.82(3)$ deg.	
	$c = 10.245(2)$ Å	$\gamma = 72.29(3)$ deg.	
Volume	$759.8(3)$ Å ³		
Z, Calculated density	2, 1.614 Mg/ m ³		
Absorption coefficient	0.136 mm ⁻¹		
F(000)	374		
Crystal size	0.50 x 0.21 x 0.17 mm		
Theta range for data collection	2.55 to 27.48 deg.		
Limiting indices	$-10 \leq h \leq 10, -10 \leq k \leq 12, -13 \leq l \leq 9$		
Reflections collected / unique	6813 / 3406 [R(int) = 0.0388]		
Completeness to theta = 27.48	97.9 %		
Absorption correction	Semi-empirical from equivalents		
Max. and min. transmission	1.0000 and 0.6693		
Refinement method	Full-matrix least-squares on F ²		
Data / restraints / parameters	3406 / 0 / 244		
Goodness-of-fit on F ²	1.120		
Final R indices [I>2sigma(I)]	R1 = 0.0677, wR2 = 0.1663		
R indices (all data)	R1 = 0.0824, wR2 = 0.1797		
Largest diff. peak and hole	0.267 and -0.395 e. Å ⁻³		

Table S2-2. Atomic coordinates ($\times 10^4$) and equivalent isotropic displacement parameters ($\text{\AA}^2 \times 10^3$) for **1**. U(eq) is defined as one third of the trace of the orthogonalized U_{ij} tensor.

	x	y	z	U(eq)
F(1)	-3639(2)	2349(2)	1643(1)	41(1)
F(2)	-2760(2)	4814(2)	-41(1)	43(1)
F(3)	-849(2)	6042(2)	862(1)	38(1)
F(4)	166(2)	4899(2)	3491(1)	36(1)
O(1)	-3398(2)	-1517(2)	6310(2)	39(1)
O(2)	283(3)	1044(2)	8100(2)	46(1)
C(1)	-2653(3)	-847(2)	6708(2)	28(1)
C(2)	-2164(3)	-1361(3)	8159(2)	32(1)
C(3)	-1247(3)	-732(3)	8607(2)	32(1)
C(4)	-643(3)	545(2)	7693(2)	29(1)
C(5)	-1193(3)	1168(2)	6236(2)	23(1)
C(6)	-727(3)	2398(2)	5367(2)	26(1)
C(7)	-1221(3)	2995(2)	3984(2)	24(1)
C(8)	-773(3)	4259(2)	3057(2)	26(1)
C(9)	-1276(3)	4836(2)	1739(2)	29(1)
C(10)	-2259(3)	4185(3)	1268(2)	30(1)
C(11)	-2701(3)	2958(3)	2118(2)	29(1)
C(12)	-2213(3)	2325(2)	3508(2)	24(1)
C(13)	-2675(3)	1064(2)	4422(2)	25(1)
C(14)	-2168(3)	492(2)	5763(2)	24(1)
C(15)	-6215(3)	2492(3)	-3478(3)	35(1)
C(16)	-5864(3)	1797(3)	-2131(3)	41(1)
C(17)	-4868(3)	2297(3)	-1474(3)	41(1)
C(18)	-4266(3)	3487(3)	-2179(2)	37(1)
C(19)	-4616(3)	4265(2)	-3599(2)	27(1)
C(20)	-5608(3)	3753(2)	-4263(2)	29(1)
C(21)	-5961(3)	4496(3)	-5651(2)	30(1)

Table S2-3. Bond lengths [\AA] and angles [deg] for **1**.

Bond lengths [\AA]	Angles [deg]
F(1)-C(11)	1.343(2)
F(2)-C(10)	1.348(2)
F(3)-C(9)	1.345(2)
F(4)-C(8)	1.341(2)
O(1)-C(1)	1.220(3)
O(2)-C(4)	1.215(3)
C(1)-C(2)	1.480(3)
C(1)-C(14)	1.489(3)
C(2)-C(3)	1.327(3)
C(2)-H(2)	0.9500
C(3)-C(4)	1.481(3)
C(3)-H(3)	0.9500
C(4)-C(5)	1.498(3)
C(5)-C(6)	1.375(3)
C(5)-C(14)	1.414(3)
C(6)-C(7)	1.414(3)
C(6)-H(6)	0.9500
C(7)-C(8)	1.413(3)
C(7)-C(12)	1.422(3)
C(8)-C(9)	1.357(3)
C(9)-C(10)	1.400(3)
C(10)-C(11)	1.357(3)
C(11)-C(12)	1.419(3)
C(12)-C(13)	1.411(3)
C(13)-C(14)	1.379(3)
C(13)-H(13)	0.9500
C(15)-C(16)	1.355(4)
C(15)-C(20)	1.434(3)
C(15)-H(15)	0.9500
C(16)-C(17)	1.422(4)
C(16)-H(16)	0.9500
C(17)-C(18)	1.359(4)
C(17)-H(17)	0.9500
C(18)-C(19)	1.431(3)

Bond lengths [Å]	Angles [deg]
C(18)-H(18)	0.9500
C(19)-C(21)#1	1.395(3)
C(19)-C(20)	1.432(3)
C(20)-C(21)	1.397(3)
C(21)-C(19)#1	1.395(3)
C(21)-H(21)	0.9500
O(1)-C(1)-C(2)	120.9(2)
O(1)-C(1)-C(14)	122.0(2)
C(2)-C(1)-C(14)	117.2(2)
C(3)-C(2)-C(1)	122.7(2)
C(3)-C(2)-H(2)	118.7
C(1)-C(2)-H(2)	118.7
C(2)-C(3)-C(4)	122.4(2)
C(2)-C(3)-H(3)	118.8
C(4)-C(3)-H(3)	118.8
O(2)-C(4)-C(3)	121.4(2)
O(2)-C(4)-C(5)	121.6(2)
C(3)-C(4)-C(5)	116.93(19)
C(6)-C(5)-C(14)	120.70(19)
C(6)-C(5)-C(4)	118.99(19)
C(14)-C(5)-C(4)	120.31(19)
C(5)-C(6)-C(7)	119.9(2)
C(5)-C(6)-H(6)	120.1
C(7)-C(6)-H(6)	120.1
C(8)-C(7)-C(6)	121.7(2)
C(8)-C(7)-C(12)	118.69(19)
C(6)-C(7)-C(12)	119.60(19)
F(4)-C(8)-C(9)	119.47(19)
F(4)-C(8)-C(7)	119.31(18)
C(9)-C(8)-C(7)	121.2(2)
F(3)-C(9)-C(8)	121.0(2)
F(3)-C(9)-C(10)	118.76(19)
C(8)-C(9)-C(10)	120.26(19)
F(2)-C(10)-C(11)	121.3(2)
F(2)-C(10)-C(9)	118.24(19)

Bond lengths [Å]	Angles [deg]
C(11)-C(10)-C(9)	120.5(2)
F(1)-C(11)-C(10)	119.38(19)
F(1)-C(11)-C(12)	119.49(19)
C(10)-C(11)-C(12)	121.1(2)
C(13)-C(12)-C(11)	122.4(2)
C(13)-C(12)-C(7)	119.36(18)
C(11)-C(12)-C(7)	118.24(19)
C(14)-C(13)-C(12)	120.1(2)
C(14)-C(13)-H(13)	119.9
C(12)-C(13)-H(13)	119.9
C(13)-C(14)-C(5)	120.35(19)
C(13)-C(14)-C(1)	119.37(19)
C(5)-C(14)-C(1)	120.27(19)
C(16)-C(15)-C(20)	120.9(2)
C(16)-C(15)-H(15)	119.6
C(20)-C(15)-H(15)	119.6
C(15)-C(16)-C(17)	120.4(2)
C(15)-C(16)-H(16)	119.8
C(17)-C(16)-H(16)	119.8
C(18)-C(17)-C(16)	120.7(2)
C(18)-C(17)-H(17)	119.6
C(16)-C(17)-H(17)	119.6
C(17)-C(18)-C(19)	120.9(2)
C(17)-C(18)-H(18)	119.5
C(19)-C(18)-H(18)	119.5
C(21)#1-C(19)-C(18)	122.5(2)
C(21)#1-C(19)-C(20)	119.2(2)
C(18)-C(19)-C(20)	118.3(2)
C(21)-C(20)-C(19)	119.2(2)
C(21)-C(20)-C(15)	122.0(2)
C(19)-C(20)-C(15)	118.8(2)
C(19)#1-C(21)-C(20)	121.6(2)
C(19)#1-C(21)-H(21)	119.2
C(20)-C(21)-H(21)	119.2

Table S2-4. Anisotropic displacement parameters ($\text{\AA}^2 \times 10^3$) for **1**. The anisotropic displacement factor exponent takes the form: $-2 \pi^2 [h^2 a^{*2} U^{11} + \dots + 2 h k a^{*} b^{*} U^{12}]$

	U11	U22	U33	U23	U13	U12
F(1)	48(1)	51(1)	31(1)	-7(1)	-9(1)	-24(1)
F(2)	52(1)	47(1)	23(1)	0(1)	-8(1)	-13(1)
F(3)	47(1)	29(1)	29(1)	2(1)	4(1)	-13(1)
F(4)	45(1)	33(1)	35(1)	-5(1)	-4(1)	-20(1)
O(1)	47(1)	36(1)	38(1)	-5(1)	-4(1)	-22(1)
O(2)	59(1)	55(1)	30(1)	-3(1)	-12(1)	-31(1)
C(1)	27(1)	25(1)	29(1)	-5(1)	2(1)	-5(1)
C(2)	36(1)	26(1)	27(1)	-1(1)	1(1)	-8(1)
C(3)	38(1)	30(1)	21(1)	-1(1)	-3(1)	-7(1)
C(4)	30(1)	29(1)	25(1)	-5(1)	-3(1)	-6(1)
C(5)	24(1)	22(1)	21(1)	-6(1)	-1(1)	-3(1)
C(6)	28(1)	25(1)	25(1)	-9(1)	-1(1)	-8(1)
C(7)	24(1)	22(1)	24(1)	-6(1)	1(1)	-5(1)
C(8)	29(1)	25(1)	27(1)	-9(1)	1(1)	-9(1)
C(9)	31(1)	23(1)	25(1)	-2(1)	4(1)	-6(1)
C(10)	33(1)	31(1)	19(1)	-3(1)	-2(1)	-3(1)
C(11)	29(1)	33(1)	25(1)	-9(1)	-4(1)	-9(1)
C(12)	25(1)	24(1)	20(1)	-5(1)	0(1)	-4(1)
C(13)	25(1)	26(1)	25(1)	-9(1)	-1(1)	-6(1)
C(14)	24(1)	22(1)	24(1)	-7(1)	1(1)	-5(1)
C(15)	34(1)	30(1)	42(1)	-14(1)	4(1)	-11(1)
C(16)	40(1)	33(1)	41(1)	-7(1)	11(1)	-8(1)
C(17)	44(2)	37(1)	28(1)	-6(1)	1(1)	3(1)
C(18)	36(1)	38(1)	33(1)	-11(1)	-4(1)	-3(1)
C(19)	26(1)	27(1)	28(1)	-11(1)	0(1)	-2(1)
C(20)	24(1)	25(1)	35(1)	-10(1)	3(1)	-4(1)
C(21)	27(1)	31(1)	33(1)	-13(1)	-4(1)	-6(1)

Table S2-5. Hydrogen coordinates ($\times 10^4$) and isotropic displacement parameters ($\text{\AA}^2 \times 10^3$) for **1**

	x	y	z	U(eq)
H(2)	-2521	-2174	8796	38
H(3)	-967	-1115	9550	38
H(6)	-74	2846	5695	31
H(13)	-3336	609	4112	30
H(15)	-6872	2140	-3908	42
H(16)	-6286	970	-1623	49
H(17)	-4620	1794	-531	49
H(18)	-3605	3807	-1722	44
H(21)	-6608	4149	-6095	36

Table S2-6. Torsion angles [deg] for **1**.

O(1)-C(1)-C(2)-C(3)	174.9(2)
C(14)-C(1)-C(2)-C(3)	-3.9(3)
C(1)-C(2)-C(3)-C(4)	0.4(4)
C(2)-C(3)-C(4)-O(2)	-175.2(2)
C(2)-C(3)-C(4)-C(5)	3.3(3)
O(2)-C(4)-C(5)-C(6)	-4.4(3)
C(3)-C(4)-C(5)-C(6)	177.0(2)
O(2)-C(4)-C(5)-C(14)	175.2(2)
C(3)-C(4)-C(5)-C(14)	-3.3(3)
C(14)-C(5)-C(6)-C(7)	-0.2(3)
C(4)-C(5)-C(6)-C(7)	179.45(18)
C(5)-C(6)-C(7)-C(8)	179.86(19)
C(5)-C(6)-C(7)-C(12)	0.7(3)
C(6)-C(7)-C(8)-F(4)	1.0(3)
C(12)-C(7)-C(8)-F(4)	-179.84(18)
C(6)-C(7)-C(8)-C(9)	-178.9(2)
C(12)-C(7)-C(8)-C(9)	0.2(3)
F(4)-C(8)-C(9)-F(3)	-0.1(3)
C(7)-C(8)-C(9)-F(3)	179.81(19)
F(4)-C(8)-C(9)-C(10)	-179.85(19)
C(7)-C(8)-C(9)-C(10)	0.1(3)
F(3)-C(9)-C(10)-F(2)	-1.1(3)
C(8)-C(9)-C(10)-F(2)	178.66(19)
F(3)-C(9)-C(10)-C(11)	179.3(2)
C(8)-C(9)-C(10)-C(11)	-0.9(3)
F(2)-C(10)-C(11)-F(1)	0.7(3)
C(9)-C(10)-C(11)-F(1)	-179.74(19)
F(2)-C(10)-C(11)-C(12)	-178.12(19)
C(9)-C(10)-C(11)-C(12)	1.5(4)
F(1)-C(11)-C(12)-C(13)	0.2(3)
C(10)-C(11)-C(12)-C(13)	179.0(2)
F(1)-C(11)-C(12)-C(7)	-179.92(19)
C(10)-C(11)-C(12)-C(7)	-1.1(3)
C(8)-C(7)-C(12)-C(13)	-179.85(19)
C(6)-C(7)-C(12)-C(13)	-0.6(3)

C(8)-C(7)-C(12)-C(11)	0.3(3)
C(6)-C(7)-C(12)-C(11)	179.47(19)
C(11)-C(12)-C(13)-C(14)	180.0(2)
C(7)-C(12)-C(13)-C(14)	0.1(3)
C(12)-C(13)-C(14)-C(5)	0.4(3)
C(12)-C(13)-C(14)-C(1)	-179.42(18)
C(6)-C(5)-C(14)-C(13)	-0.4(3)
C(4)-C(5)-C(14)-C(13)	180.00(19)
C(6)-C(5)-C(14)-C(1)	179.45(19)
C(4)-C(5)-C(14)-C(1)	-0.2(3)
O(1)-C(1)-C(14)-C(13)	4.8(3)
C(2)-C(1)-C(14)-C(13)	-176.43(19)
O(1)-C(1)-C(14)-C(5)	-175.1(2)
C(2)-C(1)-C(14)-C(5)	3.7(3)
C(20)-C(15)-C(16)-C(17)	-0.7(4)
C(15)-C(16)-C(17)-C(18)	0.7(4)
C(16)-C(17)-C(18)-C(19)	-0.1(4)
C(17)-C(18)-C(19)-C(21)#1	179.0(2)
C(17)-C(18)-C(19)-C(20)	-0.4(3)
C(21)#1-C(19)-C(20)-C(21)	0.7(3)
C(18)-C(19)-C(20)-C(21)	-179.9(2)
C(21)#1-C(19)-C(20)-C(15)	-179.1(2)
C(18)-C(19)-C(20)-C(15)	0.3(3)
C(16)-C(15)-C(20)-C(21)	-179.6(2)
C(16)-C(15)-C(20)-C(19)	0.2(3)
C(19)-C(20)-C(21)-C(19)#1	-0.7(4)
C(15)-C(20)-C(21)-C(19)#1	179.1(2)

References

1. Chen, Z.; Swager, T. M. *Org. Lett.* **2007**, *9*, 997.
2. Pommerehne, J.; Vestweber, H.; Guss, W.; Mahrt, R. F.; Bassler, H.; Porsch, M.; Daub, J. *Adv. Mater.* **1995**, *7*, 551.
3. Sun, Q.; Wang, H.; Yang, C.; Li, Y. *J. Mater. Chem.* **2003**, *13*, 800.
4. (a) Becke, A. D. *Phys. Rev. A* **1988**, *38*, 3098. (b) Lee, C.; Yang, W.; Parr, G. G. *Phys. Rev. B* **1988**, *37*, 785.
5. Frisch, M. J.; Trucks, G. W.; Schlegel, H. B.; Scuseria, G. E.; Robb, M. A.; Cheeseman, J. R.; Montgomery, J. A. Jr.; Vreven, T.; Kudin, K. N.; Burant, J. C.; Millam, J. M.; Iyengar, S. S.; Tomasi, J.; Barone, V.; Mennucci, B.; Cossi, M.; Scalmani, G.; Rega, N.; Petersson, G. A.; Nakatsuji, H.; Hada, M.; Ehara, M.; Toyota, K.; Fukuda, R.; Hasegawa, J.; Ishida, M.; Nakajima, T.; Honda, Y.; Kitao, O.; Nakai, H.; Klene, M.; Li, X.; Knox, J. E.; Hratchian, H. P.; Cross, J. B.; Adamo, C.; Jaramillo, J.; Gomperts, R.; Stratmann, R. E.; Yazyev, O.; Austin, A. J.; Cammi, R.; Pomelli, C.; Ochterski, J. W.; Ayala, P. Y.; Morokuma, K.; Voth, G. A.; Salvador, P.; Dannenberg, J. J.; Zakrzewski, V. G.; Dapprich, S.; Daniels, A. D.; Strain, M. C.; Farkas, O.; Malick, D. K.; Rabuck, A. D.; Raghavachari, K.; Foresman, J. B.; Ortiz, J. V.; Cui, Q.; Baboul, A. G.; Clifford, S.; Cioslowski, J.; Stefanov, B. B.; Liu, G.; Liashenko, A.; Piskorz, P.; Komaromi, I.; Martin, R. L.; Fox, D. J.; Keith, T.; Al-Laham, M. A.; Peng, C. Y.; Nanayakkara, A.; Challacombe, M.; Gill, P. M. W.; Johnson, B.; Chen, W.; Wong, M. W.; Gonzalez, C.; Pople, J. A. *Gaussian 03*, Revision C.02; Gaussian Inc.: Wallingford CT, 2004.
6. Dennington, R., II; Keith, T.; Millam, J.; Eppinnett, K.; Hovell, W. L.; Gilliland, R. *GaussView*, Version 3.09; Semichem, Inc.: Shawnee Mission, KS, 2003.
7. Rowland, R. S.; Taylor, R. *J. Phys. Chem.* **1996**, *100*, 7384.